Optica Applicata, Vol. XL, No. 3, 2010

Multiwavelength micropulse lidar for atmospheric aerosol investigation

MICHAŁ POSYNIAK[1*], TADEUSZ STACEWICZ[2], MACIEJ MIERNECKI[1], ANNA K. JAGODNICKA[2], SZYMON P. MALINOWSKI[1]

[1]Atmospheric Physics Division, Institute of Geophysics, University of Warsaw, ul. Pasteura 7, 02-093 Warsaw, Poland

[2]Optics Division, Institute of Experimental Physics, University of Warsaw, ul. Hoża 69, 00-681 Warsaw, Poland

[*]Corresponding author: mpos@igf.fuw.edu.pl

Multiwavelength micropulse lidar (MML) designed for continuous atmospheric sounding is presented. In its optical emitter, a diode pumped pulsed Nd:YAG laser is used. The laser generates three wavelengths: 1064, 532 and 355 nm. Energies of light pulses are about 30, 15 and 7 μJ, respectively, while their repetition rate is 2 kHz. Returning light is collected by a Cassegrain telescope with the mirror of 170 mm in diameter. Then, the signal is spectrally separated by a polichromator built with dielectric interference and colour filters. Detection of the signals is performed with three photomultipliers and a multiscaling photon counter. Preliminary results of investigation of aerosol properties during COAST 2009 experiment on the Baltic Sea are presented.

Keywords: micropulse lidar, atmospheric aerosol, optical teledetection.

1. Introduction

Lidar techniques are commonly used for remote sensing of the atmosphere and environmental monitoring. They are often applied for atmospheric aerosol investigation and cloud observations. This remote sensing instrument emits the light pulses and then measures properties of the radiation scattered back by distant objects. Measuring the time delay between the emitted pulse and the echo signal enables us to estimate the range to the object. The analysis of the properties of the lidar returns provides opportunity to retrieve information about scattering objects.

Commonly in the lidars, the flash-lamp pumped lasers generating light pulses of 0.1–1 J energy at repetition rate 10–100 Hz [1] are installed. Such lasers are not suitable for permanent measurements due to the high cost of service and high maintenance requirements. A typical lifetime of their flash-lamps reaches millions of shots, so with increasing the repetition frequency their working time without the service decreases, running down only to few week long period. Also the lifetime of electronic

devices working under high voltage and at strong pulse regime (thyristors, capacitors, *etc*.) is limited. Additionally, high power lasers cause problems due to degeneration of mirrors, harmonic crystals and other optical elements, which need to be exchanged as well.

A micropulse lidar is an interesting alternative for high energy lidars. It was described for the first time by CAMPBELL *et al*. [2]. In these constructions, the high repetition rate micropulse diode pumped lasers or even the diode lasers are applied. By now the lifetime of such diodes runs into thousands of hours and they consume relatively little power. Due to that, they are safer in operation and can be used for permanent measurements. Such lidars are compact and can be easily installed in any place [3].

However, low energy of the light pulses from such lasers, which is typically about 3–4 orders of magnitude less than the energy of the lamp pumped lasers, causes the lidar returns weak. Detection and recording of such signals require the usage of the most sensitive techniques, *i.e*., the time-dependent photon counting (multiscaling) [4]. Then, the low signal strength is compensated by a high pulse repetition rate: usually of 1–10 kHz, which allows to achieve a good signal to noise ratio due to efficient signal averaging.

In this paper we present a prototype multiwavelength micropulse lidar (MML) designed for continuous sounding of the atmosphere. Such investigation is important because it allows to collect the climatologically significant data about optical properties of atmospheric aerosols.

Almost all of currently operating micropulse lidars work with one wavelength [3]. To our knowledge, a 3-wavelength micropulse lidar was presented only by ZAVYALOV *et al*. [5]. The investigation into several wavelengths provides more complete information about the atmosphere. It enables retrieving the aerosol characteristics, not obtainable by other techniques, like particle size distributions.

2. Instrumentation

A scheme of our MML is presented in Fig. 1. In the lidar transmitter, the diode-pumped pulsed Nd:YAG laser (DTL-374QT) from Laser-export Co. Ltd. is installed. It generates radiation at three harmonics (1064, 532 and 355 nm). Energies of light pulses are about 30, 15 and 7 μJ, respectively. Their FWHM time is about 6 ns and the repetition rate can be tuned in a range from 200 Hz up to 10 kHz. Tests showed that the optimal pulse power is achieved with the repetition rate of 2 kHz.

Beams of all harmonics are emitted coaxially and are strongly divergent (about 7 mrad). In order to match this parameter with the observation angle of the telescope used in the optical receiver (~1 mrad), a beam expander was applied (Fig. 1). It was constructed with mirrors, due to minimal chromatic aberration of this solution. Divergent laser beams are collimated using broadband dielectric mirror M1 (0.5 m focal length) and send to the atmosphere using second flat mirror M2. The expander widens the initial diameter of the beams to approximately 1.5 cm and reduces their

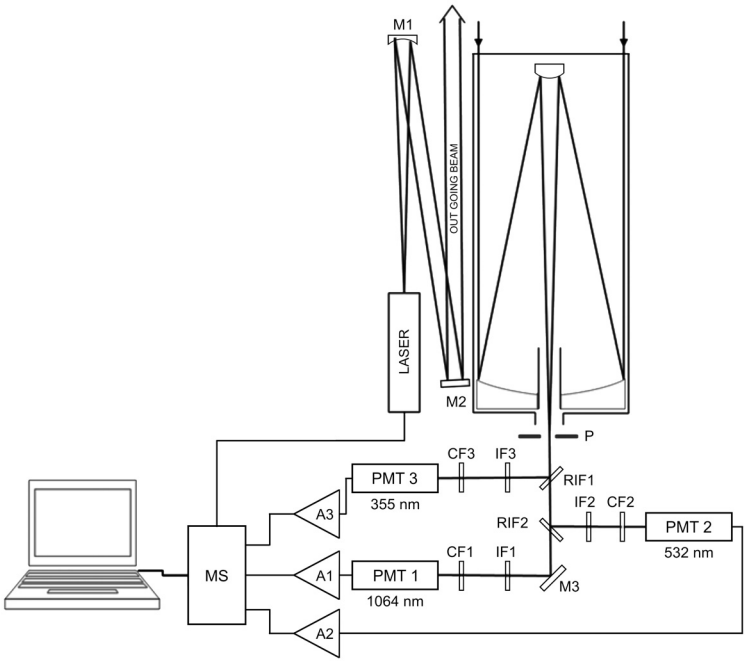

Fig. 1. Scheme of MML (description in the text).

residual divergence to approximately 0.3 mrad. Correct work of the expander is possible due to the fact that divergence of all beams is similar and their virtual sources are located at approximately the same distance from the mirror M1.

In the optical receiver, a Cassegrain telescope with the mirror of 170 mm in diameter is used. Focal length of the telescope is about 2.7 m. Collected light is spectrally separated by a polichromator consisting of wavelength selective dielectric mirrors (RIF1, RIF2) which direct appropriate harmonics to the respective PMTs. In order to eliminate optical crosstalk between the channels, the PMTs are blocked by narrowband ($\Delta\lambda$ = 10 nm – CVI) interference filters (IF1–IF3) whose transmission bandpass is matched to wavelengths emitted by the transmitter. The IF filters selectivity is additionally enhanced by colour filters (CF1–CF3). Registration of the signals is done with three photomultipliers: Hamamatsu R316-02P for detection at 1064 nm channel, EMI 9558QB at 532 nm and EMI 9807B for 355 nm. Construction of the receiver is compact enough to avoid using the collimating lenses. Due to long telescope focal length and short light paths inside the polichromator (< 19 cm), the size of the respective beams is less than 12 mm, so they are well collected by the photomultipliers, whose input aperture is about 1 inch.

The acquisition of amplified PMT signals (A1–A3) is performed with photon counting technique. A four channel digital multiscaler (MS) was dedicated to this lidar system and designed in collaboration with ARCO Company (Kraków, Poland). The multiscaler is conformed for registration with a high repetition rate of trigger

pulses (2 kHz). Each channel contains a record of 2048 bins controlled by 50 MHz internal clock what corresponds to 20 ns temporal resolution. Numbers of counts registered in the records are transferred to the computer via USB 2.0 interface, where they are subsequently averaged over a certain number of laser pulses.

The record length of 2048 bins, which is used in the present setup, enables the lidar registrations up to 6 km. Initial measurements proved that the range up to 12 km is possible, with the record length increased to 4096 bins.

Although the full overlap distance of the emitter–receiver system starts at 200 m [6], the dead zone of MML is longer and reaches about 750 m due to photonic pulses which overlap at a short distance of signals in the photon counting mode [4].

The lidar mount allows to set any elevation angle of observation.

3. Signal analysis

A preliminary test of our lidar system was performed during COAST 2009. The goal of this campaign was to look for contrasts in properties of marine and land aerosol. Land lidar stations in Sopot (ceiliometer from Institute of Geophysics, University of Warsaw, Poland) and in Władysławowo (lidar from Institute of Oceanology, Polish Academy of Sciences) were involved in the experiment. The MML was installed in the laboratory on board of the research vessel r/v Oceania. In the following part we present preliminary analysis of the data collected on September 29, 2009. At this time the research vessel was on the position of approximately 54°49′ N and 18°45′ E, about 14 km from Hel Peninsula. The wind speed was about 10 m/s, blowing from SW. The laser beam was sent on starboard side at an elevation angle of 45°. Measurements were performed in stable conditions what allowed the long averaging of the signals (30 min).

In Figure 2, examples of lidar signals are shown. Malfunctioning 1064 nm channel was excluded from the analysis, so only the data from 532 nm and 355 nm channels are discussed.

Commonly ideal lidar signals are described by equation [7]:

$$S_{0\lambda}(z) = \frac{A_\lambda}{(z-z_0)^2}\,\beta_\lambda(z)\exp\left(-2\int_{z_0}^{z}\alpha_\lambda(y)\mathrm{d}y\right) \tag{1}$$

Here z denotes the distance from the lidar, and z_0 is the lidar position, while λ is the lidar wavelength, A_λ are the apparatus constants, $\alpha_\lambda(z)$ and $\beta_\lambda(z)$ are total atmospheric extinction and backscattering coefficients, respectively. The analysis of lidar signals provides an opportunity to retrieve these coefficients, containing important information about properties of atmosphere. In order to reduce uncertainties due to noise caused by photon number fluctuations and interferences, a special procedure resulting in a significant signal to noise ratio improvement was introduced.

Random electric noise and fluctuations of photon numbers are usually reduced by averaging the data over a certain number of laser pulses n. In this way,

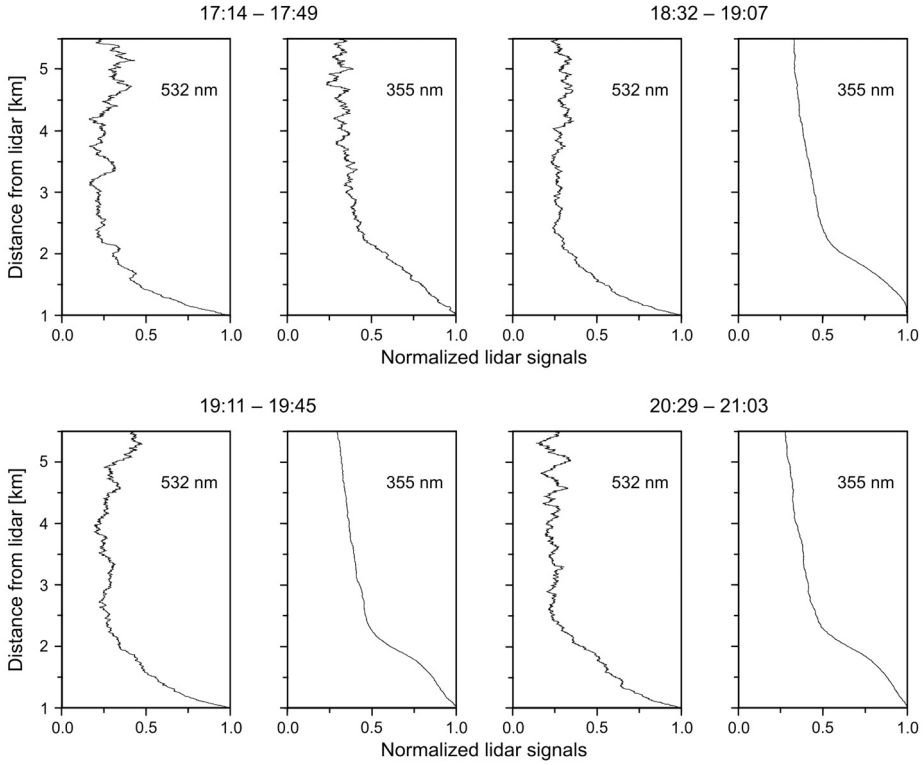

Fig. 2. Examples of lidar signals collected on September 29, 2009.

the improvement of the signal to noise ratio (S/N) by a factor of $\sqrt{n}$ is achieved [8]. However, it also leads to reduction of the temporal resolution of the data (30 min in our case). Such averaging does not eliminate the interferences resulting from the photomultiplier dark counts and from a photonic background. This is manifested by the offset of the signal. For each wavelength, the raw signals affected by the offset might be expressed by:

$$S_\lambda(z) = O_\lambda + S_{\lambda 0}(z) \tag{2}$$

where $S_{\lambda 0}$ denotes the pure lidar return. Assuming that the mean value of the offset O_λ does not change with the distance and converting (2) to, the so-called, "range corrected" form [7], one achieves:

$$L_\lambda(z) = (z - z_0)^2 S_\lambda(z) = (z - z_0)^2 O_\lambda + (z - z_0)^2 S_{\lambda 0}(z) = (z - z_0)^2 O_\lambda + L_{\lambda 0}(z) \tag{3}$$

The equation consists of the constituent describing the offset and the pure, range corrected lidar return $L_{\lambda 0}(z)$. At large distances $L_{\lambda 0}(z)$ decreases to zero while the offset term that is square dependent on $z_0 - z$, strongly dominates. Then, with a fit

of the square function at large distances, the value of O_λ might be easily determined and eliminated [9].

Further reduction of random electric noise and fluctuations of photon numbers can be done by smoothing the signals over a certain number of bins p. It improves S/N ratio by a factor of $\sqrt{p}$ but also decreases the spatial resolution of the lidar by a factor of p [8]. The signal smoothing can be performed in several ways, from the simplest like adjacent averaging (running mean) to weighed methods like Gaussian smoothing [10]. According to formula (1), the lidar signal decreases quickly with increasing distance. This pushed us to elaborate a technique of p number selection. The lidar signal was divided into intervals of $w = 10$ bins. For each interval the mean signal value M and the standard deviation D was calculated and D/M as a function of distance z was plot. These values were interpreted as a measure of noise and fluctuations. Then, the function, called by us dev(z), was fit to these data points. Finally, taking into account the root dependence between p and S/N ratio, p-number was determined according to formula:

$$p(z) = a\left[\mathrm{dev}(z)\right]^2 + b \tag{4}$$

where a and b are constants. In our case p usually changed from 10 bins close to the lidar to 100 bins at the end of the signal range. Such procedure leads to the efficient increase and stabilization of a signal to noise ratio along the distance with gradually decreasing spatial resolution.

After the elimination of the offset and improvement of S/N, the recorded signals were used to retrieve aerosol optical properties. Klett–Fernald method was applied [11]. It allows to solve the lidar equation and to determine the aerosol backscattering coefficient using assumptions of linearity between the backscattering and the extinction coefficients. For aerosol:

$$\beta_{\lambda A} = R_{\lambda A}\alpha_{\lambda A} \tag{5}$$

where $R_{\lambda A}$ denotes, the so-called, inverted lidar ratio. Similarly, for the light scattering on atmospheric molecules:

$$\beta_{\lambda R} = R_{\lambda R}\alpha_{\lambda R} \tag{6}$$

The parameters $\alpha_{\lambda R}(z)$ and $\beta_{\lambda R}(z)$ might be calculated from Rayleigh theory of light scattering in standard atmosphere [12, 13]. While $\alpha_\lambda = \alpha_{\lambda A} + \alpha_{\lambda R}$ and $\beta_\lambda = \beta_{\lambda A} + \beta_{\lambda R}$ one can substitute the relations (5) and (6) to the equation (1). Converting it to the range corrected form, we achieve:

$$L_{\lambda 0}(z) = A_\lambda\left[\beta_{\lambda A}(z) + \beta_{\lambda R}(z)\right]\exp\left(-\frac{2}{R_{\lambda A}}\int_{z_0}^{z}\beta_{\lambda A}(x)\mathrm{d}x\right)\exp\left(-\frac{2}{R_{\lambda A}}\int_{z_0}^{z}\beta_{\lambda R}(x)\mathrm{d}x\right) \tag{7}$$

The lidar signals are quantized in space with the interval Δz resulting from the digitization rate and smoothing procedure. At a distance z_n for each wavelength, the signals can by expressed by:

$$L_{\lambda 0}(z_n) = A_\lambda \left[\beta_{\lambda A}(z_n) + \beta_{\lambda R}(z_n)\right] \exp\left(-\frac{2\Delta z}{R_{\lambda A}} \sum_{i=0}^{n} \beta_{\lambda A}(z_i)\right) T_{\lambda R}(z_n) \tag{8}$$

where n denotes the altitude point index and:

$$T_{\lambda R}(z_n) = \exp\left(-\int_0^{z_n} \alpha_{\lambda R}\, \mathrm{d}r\right) \tag{9}$$

Then, the discrete form of backscatter coefficient calculated by Klett–Fernald method gets the form:

$$\beta_{\lambda A}(z_{n-1}) = \frac{A}{B + C} - D \tag{10}$$

where

$$A = L_{\lambda 0}(z_{n-1}) T_{\lambda R}^{2(\gamma_\lambda - 1)}(z_{n-1})$$

$$B = \frac{L_{\lambda 0}(z_n) T_{\lambda R}^{2(\gamma_\lambda - 1)}(z_{n-1})}{\beta_{\lambda R}(z_n) + \beta_{\lambda A}(z_n)}$$

$$C = \frac{\Delta z}{R_{\lambda A}} \left[L_{\lambda 0}(z_n) T_{\lambda R}^{2(\gamma_\lambda - 1)}(z_n) - L_{\lambda 0}(z_{n-1}) T_{\lambda R}^{2(\gamma_\lambda - 1)}(z_{n-1})\right]$$

$$D = \beta_{\lambda R}(z_{n-1})$$

while

$$\gamma_\lambda = \frac{R_{\lambda R}}{R_{\lambda A}} \tag{11}$$

Usually, the calculation is done in a backward direction starting from the most distant point $z_{n\,\max}$. However, there are no startup parameters in the above algorithm, *i.e.*, the value of $R_{\lambda A}$, the backscatter coefficient at the farthest point $\beta_{\lambda A}(z_{n\,\max})$. Therefore, the starting altitude was picked at 4 km, where the aerosol extinction was assumed negligible. The parameter $R_{\lambda A}$ was determined using normalization of

lidar data to the aerosol optical thickness τ_λ registered by means of a sunphotometer [14–16]:

$$R_{\lambda A} = \frac{\int \beta_{\lambda A}(n)\mathrm{d}z}{\tau_\lambda} \tag{12}$$

The determination of $R_{\lambda A}$ was done with the iteration method. First the starting value of this parameter was substituted to (10) and the right-hand side integral in the above equation was calculated. In this way, the new value of $R_{\lambda A}$ was found. This convergent procedure was repeated until the stable value of $R_{\lambda A}$ was achieved.

Plots in Fig. 3 show examples of atmospheric extinction inverted from lidar signals. Dot lines correspond to extinction due to Rayleigh scattering [12, 13].

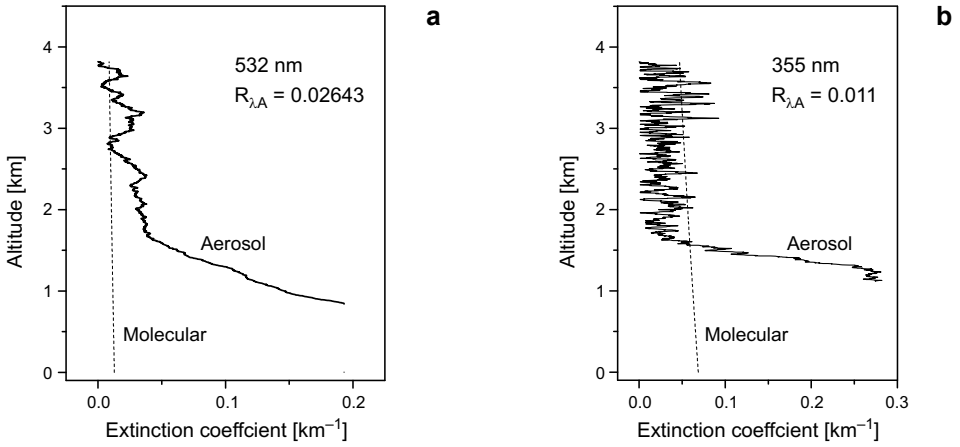

Fig. 3. Examples of aerosol extinction retrieved from MML signals during COAST 2009 at September 27, 2009 (solid line).

One can observe that the region of high extinction due to aerosol is located up to approximately 1.5 km height, which corresponds to the depth of the planetary boundary layer (PBL) height [15]. Accumulation of aerosols within PBL, under the inversion layer which suppressed vertical mixing, is a typical atmospheric phenomenon. The depth of the boundary layer observed with the lidar is in accordance with the independent measurement – atmospheric sounding performed by the nearby (70 km west, upwind) Łeba (Poland) aerological station.

The retrieved vertical distribution of extinction due to the presence of atmospheric aerosol, hardly available with the use of other instruments, demonstrates the applicability of the MML lidar. Such data are crucial, *e.g.*, for atmospheric dispersion and transport modeling [16–18].

The results of COAST 2009 campaign presented here are preliminary and their analysis is in progress.

4. Conclusions

Construction and preliminary results obtained with a prototype micropulse multiwavelength lidar were presented. The instrument is compact and can be easily transported, so it can be used in field campaigns as well as for permanent observations. Capabilities provided by this instrument were checked during the investigation of marine aerosol on r/v Oceania (COAST 2009 campaign). A special signal processing technique aimed at the minimization of a signal to noise ratio was applied to retrieve information on aerosol extinction. Preliminary profiles of the properties of atmospheric aerosols are in agreement with the independent meteorological information, demonstrating the ability of the instrument to deliver valuable data on the optical properties of atmospheric aerosol.

Acknowledgments – The authors would like to thank dr hab. T. Petelski and dr hab. T. Zielinski for an invitation to the COAST 2009 measurement camping, as well as L. Buller and A. Jaruga for their contribution to measurements. This work was partially supported by Anna Pasek Foundation.

References

[1] KOVALEV V.A., EICHINGER W.E., *Elastic Lidar: Theory, Practice, and Analysis Methods*, Wiley-Interscience, 2004.

[2] CAMPBELL J.R., HLAVKA D.L., WELTON E.J., FLYNN C.J., TURNER D.D., SPINHIRNE J.D., SCOTT III V.S., HWANG I.H., *Full-time, eye-safe cloud and aerosol lidar observation at atmospheric radiation measurement program sites: Instruments and data processing*, Journal of Atmospheric and Oceanic Technology **19**(4), 2002, pp. 431–442.

[3] WELTOM E.J., CAMPBELL J.R., BERKOFF T.A., VALENCIA S., SPINHIME J.D., HOLBEN B., TSAY S.-C., *The NASA Micro-Pulse Lidar NETWORK (MPLNET): Co-location of lidars with aeronet sunphotometers and related earth science applications*, 85th AMS Annual Meeting, American Meteorological Society – Combined Preprints, 2005, pp. 5165–5169.

[4] BECKER W., *Advanced Time-Correlated Single Photon Counting Techniques*, Springer, 2005.

[5] ZAVYALOV V.V., MARCHANT C., BINGHAM G.E., WILKERSON T.D., SWASEY J., ROGERS C., AHLSTROM D., TIMOTHY P., *Retrieval of physical properties of particulate emission from animal feeding operations using three-wavelength elastic lidar measurements*, Proceedings of SPIE **6299**, 2006, p. 62990S.

[6] STELMASZCZYK K., DELL'AGLIO M., CHUDZYNSKI S., STACEWICZ T., WÖSTE L., A*nalytical function for lidar geometrical compression form-factor calculations*, Applied Optics **44**(7), 2005, pp. 1323–1331.

[7] MEASURES R.M., *Laser Remote Sensing Fundamentals and Applications*, Krieger Publishing Company, 1992.

[8] OTT H.W., *Noise Reduction Techniques in Electronic Systems*, Wiley-Interscience, 1988.

[9] JAGODNICKA A.K., STACEWICZ T., KARASINSKI G., POSYNIAK M., MALINOWSKI S.P., *Particle size distribution retrieval from multiwavelength lidar signals for droplet aerosol*, Applied Optics **48**(4), 2009, pp. B8–B16.

[10] PIADLOWSKI M., SWACZYNA P., STACHLEWSKA I., *Diurnal and seasonal cycle of the planetary boundary layer over Warsaw*, OTEM 2009 Proceedings, pp. 36–39.

[11] FERNALD F.G., *Analysis of atmospheric lidar observations: Some comments*, Applied Optics **23**(5), 1984, pp. 652–653.

[12] FRÖHLICH C., SHAW G.E., *New determination of Rayleigh scattering in the terrestrial atmosphere*, Applied Optics **19**(11), 1980, pp. 1773–1775.

[13] BODHAINE B.A., WOOD N.B., DUTTON E.G., SLUSSER J.R., *On Rayleigh optical depth calculation*, Journal of Atmospheric and Oceanic Technology **16**(11), 1999, pp. 1854–1861.

[14] MORYS M., MIMS III F.M., HAGERUP S., ANDERSON S.E., BAKER A., KIA J., WALKUP T., *Design, calibration, and performance of MICROTOPS II handheld ozone monitor and Sun photometer*, Journal of Geophysical Research **106**(D13), 2001, pp. 14573–14582.

[15] MARKOWICZ K.M., FLATAU P.J., KARDAŚ A.E., REMISZEWSKA J., STELMASZCZYK K., WOESTE L., *Ceilometer retrieval of the boundary layer vertical aerosol extinction structure*, Journal of Atmospheric and Oceanic Technology **25**(6), 2008, pp. 928–944.

[16] KARDAS A.E., MARKOWICZ K.M., STELMASZCZYK K., KARASINSKI G., MALINOWSKI S.P., STACEWICZ T., WOESTE L., HOCHHERTZ C., *Saharan aerosol sensed over Warsaw by backscatter depolarization lidar*, Optica Applicata **40**(1), 2010, pp. 219–237.

[17] PIETRUCZUK A., CHAIKOVSKY A.P., *Properties of fire smoke in Eastern Europe measured by remote sensing methods*, Proceedings of **6745**, 2007, p. 67451T.

[18] PAPAYANNIS, A., AMIRIDIS V., MONA L., TSAKNAKIS G., BALIS D., BÖSENBERG J., CHAIKOVSKI A., DE TOMASI F., GRIGOROV I., MATTIS I., MITEV V., MÜLLER D., NICKOVIC S., PÉREZ C., PIETRUCZUK A., PISANI G., RAVETTA F., RIZI V., SICARD M., TRICKL T., WIEGNER M., GERDING M., MAMOURI R.E., D'AMICO G., PAPPALARDO G., *Systematic lidar observations of Saharan dust over Europe in the frame of EARLINET (2000–2002)*, Journal of Geophysical Research **113**, 2008, p. D10204.

Received January 5, 2010
in revised form May 27, 2010